RESEARCH

Future climate projections using the LARS-WG6 downscaling model over Upper Indus Basin, Pakistan

Summera Fahmi Khan · Usman Ali Naeem

Abstract This study investigates the projections of precipitation and temperature at the local scale in the Upper Indus Basin (UIB) in Pakistan using six Regional Climate Models (RCMs) from COR-DEX under two Representative Concentration Pathways (RCP 4.5 and RCP 8.5). For twenty-four stations spread across the study area, the Long Ashton Research Station Weather Generator, version six (LARS-WG6), was used to downscale the daily data from the six different RCMs for maximum temperature (T_{max}), minimum temperature (T_{min}), and precipitation (pr) at a spatial resolution of 0.44°. Investigations were made to predict changes in mean annual values of T_{max}, T_{min}, and precipitation during two future periods, i.e., the mid-century (2041–2070) and end-century (2071–2100). The model results from statistical and graphical comparison validated that the LARS-WG6 can simulate the temperature and the precipitation in the UIB. Each of the six RCMs and their ensemble revealed a continuously increased temperature projection in the basin; nevertheless, there is variation in projected magnitude across RCMs and between RCPs. The rise in average T_{max} and T_{min} was more significant under RCP 8.5 than RCP 4.5, possibly due to unmitigated greenhouse gas emissions (GHGs). The precipitation projections follow the non-uniform trend, i.e., not all RCMs agree on whether the precipitation will increase or decrease in the basin, and no orderly variations were detected during any future periods under any RCP. However, an overall increase in precipitation is projected by the ensemble of RCMs.

Keywords Precipitation · Temperature · CORDEX · RCPs · UIB · LARS-WG6

Introduction

The natural systems are under considerable threat because of the rise in temperatures and consequent global shifts in precipitation patterns (Barros et al., 2014). This threat will deepen, and these changes will severely affect socioeconomic systems by the end of this century (Ding et al., 2016). A global rise in temperature between 0.3 °C and 4.8 °C is predicted by the end of this century in the 5th Assessment Report (AR5) of the Intergovernmental Panel on Climate Change (IPCC) due to the emissions of greenhouse gases (GHG) (IPCC, 2013).

High-altitude areas are more fragile to climate change (Buytaert et al., 2010) and are easily affected

S. F. Khan (✉) · U. A. Naeem
University of Engineering and Technology, Taxila, Pakistan
e-mail: fahmi.wah@gmail.com

U. A. Naeem
e-mail: usman.naeem@uettaxila.edu.pk

S. F. Khan
COMSATS University Islamabad, Wah Campus, Wah Cantt, Pakistan

by climatic changes. These changes affect these regions' services, including water supply for hydropower and crop production. Mountain Research Initiative (MRI, 2015) and Gerlitz et al. (2016) predicted increased warming trends over high altitudes. These climatic changes endanger the overall hydrological equilibrium upstream and aggravate the issues associated with water management downstream. It is, therefore, of the utmost importance to investigate the likely impacts of climate change on the future water availability from the mountainous watersheds.

The upper Indus basin (UIB), as shown in Fig. 1, contributes approximately half of the surface water availability in Pakistan (Hasson et al., 2017), thereby ensuring the continued existence of the immediate downstream Tarbela reservoir, which is the primary water storage structure in the country.

Water availability strongly depends on climate projections under different greenhouse gas (GHG) emissions. Since the agricultural sector of Pakistan's economy is highly dependent on erratic water supplies from the Hindukush-Karakoram-Himalayan (HKH) watersheds of the Indus basin, it is of the utmost importance to conduct a realistic evaluation of the future water availability from these watersheds in order to ensure the socioeconomic development of the country in a sustainable manner. Therefore, an awareness of the likely variations in precipitation and temperature in UIB that may occur in the future is essential to explore the impact on water resources and livelihoods of the country. It will be helpful in the process of creating and putting into action appropriate adaptation strategies on a river basin scale.

Many researchers have used global climate models (GCMs) and representative concentration pathways
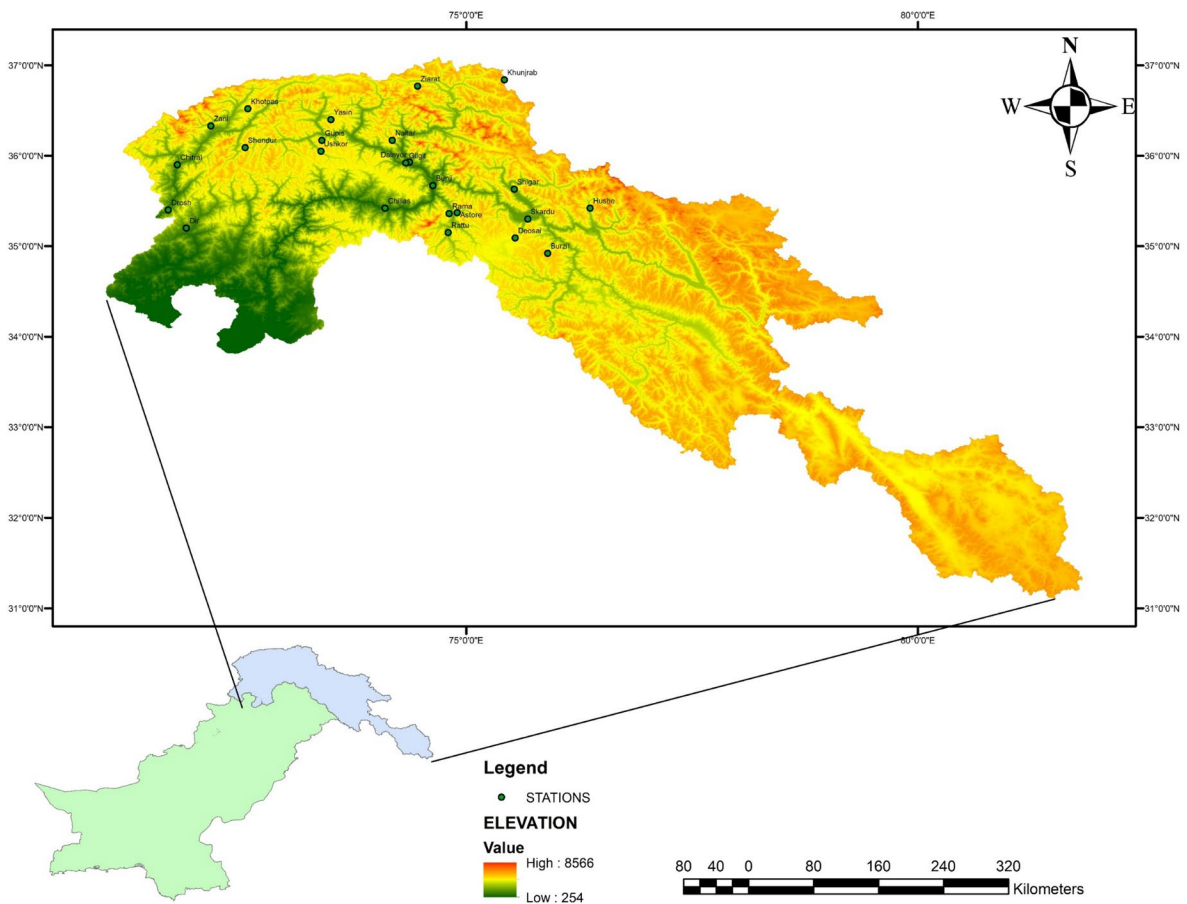

Fig. 1 Upper Indus Basin (showing meteorological stations)

(RCPs) to forecast future climate change. However, because of the relatively coarse computational cells that they use, GCMs are not suitable for direct application to sub-grid or local-scale impact studies (Fowler et al., 2007). So, these GCMs need to be downscaled either using statistical downscaling (SD) or dynamical downscaling (DD). DD can be achieved using the regional climate model (RCM) embedded in a larger GCM. RCMs use the boundary conditions of the GCMs and dynamically downscale them to the limited area of interest with more detailed output (Abiodun & Adedoyin, 2016). Because of their ability to capture weather phenomena at various spatial and temporal scales, RCMs are now widely used to simulate the future climate, assess the impacts of climate on water resources, and predict extreme hydrological events (Kim et al., 2020; Lee & Cha, 2020). The Coordinated Regional Downscaling Experiment (CORDEX) consists of many RCMs used worldwide by researchers. Bukovsky and Mearns (2020) have used a multi-model ensemble of NA-CORDEX RCMs to project temperature and precipitation. Luhunga et al. (2018) have used CORDEX RCMs to project climate changes in Tanzania. Fotso-Nguemo et al. (2019) have used a multi-model ensemble of CORDEX to predict the impact of climate change on extreme precipitation indices over Central Africa. Chapagain et al. (2021) used CORDEX-SA for the future projection of climate indices under low- and high-emission scenarios for Nepal. EURO-CORDEX and MED-CORDEX have been used by (Baronetti et al., 2022) to predict drought events in northern Italy.

RCMs may be further downscaled to the point data of gauging stations using SD techniques because it is not uncommon for meteorological stations in close proximity to exhibit different climate trends (Daly, 2006; Pepin et al., 2022). The primary reason is that a complex interplay of local and regional factors, such as topography, elevation, land use, and proximity to bodies of water, influences climate. The SD technique establishes statistical links between large-scale weather and local-scale weather. Extensive research on the downscaling of GCMs has been carried out. However, there are only a few studies on the downscaling of RCMs.

The SD techniques are among the most popular since they have the advantages of being computationally affordable and providing comprehensive station-specific data (Trzaska & Schnarr, 2014). Karam et al.

(2022) used this technique to downscale CORDEX RCM to assess hydrological extremes in the Congo basin. One example of the SD technique is the Long Ashton Research Station Weather Generator (LARS-WG6) (Semenov et al., 2002). Various researchers and studies have adopted it and shown that it can simulate future climate with reasonable skills (Hashmi et al., 2011) and (Bayatvarkeshi et al., 2020). It has been used successfully in numerous studies to downscale climate variables, such as in the Koshi River Basin in Nepal (Agarwal et al., 2014), Gujrat, India (Sarkar et al., 2015), the Nile River Basin Basin (Fenta Mekonnen & Disse, 2018), and Northeastern China (Sha et al., 2019).

Many studies have used downscaled GCMs based on various RCP scenarios for evaluating potential climate changes and their impact on UIB hydrology (Lutz et al., 2016a, 2016b; Ougahi et al., 2022; Pomee & Hertig, 2021). Few researchers have used RCMS for the Upper Indus Basin, including Hassan et al. (2019), Khan et al. (2015), and Shah et al. (2020). Among these, some have used only one RCM or a set of RCMs for the end century and only for one RCP scenario. Considering the significance of the UIB for Pakistan, conducting a more in-depth study investigating concerns regarding an uncertain future is indispensable by considering climate predictions from a more significant number of RCMs, additional RCPs, and more than one future period in the twenty-first century. In this perspective, the goals of the current research were to examine the capability of LARS-WG6 for downscaling RCMs in the UIB and, further, use the downscaled data to project the future climate changes for two selected periods, i.e., [2041–2070 (the 2050s)] and [2071–2100 (2080s)] under RCP 4.5 and RCP 8.5 scenarios. These findings will be valuable in environmental planning and risk reduction initiatives on a local scale, particularly those about water resources and extreme hydrological events.

Materials and methods

Study area description

The Indus River is one of the largest rivers in the world. It is a transboundary river spread across Pakistan, India, China, and Afghanistan. The part of the Indus up to Tarbela Dam is considered the Upper Indus Basin, which has

been used as the study area. It is a mountainous watershed with elevation ranging from 270 to 8465 m above sea level. Most of the part is covered with perennial snow. It is a significant source of fresh water for Pakistan. Since the watershed is mountainous, the gauging stations are sparse and challenging to manage. Figure 1 shows the location of gauging stations on the UIB. The importance of the Upper Indus Basin in Pakistan is evident because it provides the most considerable amount of water to the country's primary industry, i.e., agriculture. Moreover, it is considered to be a climate change hot spot by many researchers, including Nepal and Shrestha (2015), Kilroy (2015), and De Souza et al. (2015), with a tremendously uncertain future hydro-climatology.

Observed data

The gauge data of three climatic parameters, i.e., precipitation (pr), maximum temperature (T_{max}),

and minimum temperature (T_{min}) at daily time step for all the twenty-four stations of the study area has been collected from the Pakistan Meteorological Department (PMD) and Water and Power Development Authority (WAPDA). Details of gauging stations have been listed in Table 1, and the location of meteorological stations is shown in Fig. 1.

Quality control of gauge data has been done using RClimdex (Zhang & Yang, 2004), and inhomogeneities were removed using the Climatol package in R, developed by Guijarro (2017).

Regional climate model data

Regional Climate Model (RCM) data has been collected from the CORDEX-SA experiment at daily time steps from the website https://esgf-data.dkrz.de/search/esgf-dkrz/. CORDEX-SA provides several RCMs for the study area. However, six different

Sr.No	Meteorological station	Longitude	Latitude	Elevation (m)	Data period	Data providing agency
1	Astore	74.90	35.37	2168	1960–2019	PMD
2	Bunji	74.63	35.67	1372	1961–2019	PMD
3	Chillas	74.10	35.42	1250	1961–2019	PMD
4	Chitral	71.80	35.90	1498	1981–2019	PMD
5	Dir	71.90	35.20	1369	1968–2019	PMD
6	Drosh	71.70	35.40	1464	1961–2019	PMD
7	Gilgit	74.33	35.92	1460	1960–2019	PMD
8	Gupis	73.40	36.17	2156	1961–2019	PMD
9	Skardu	75.68	35.30	2210	1961–2019	PMD
10	Burzil	75.90	34.92	4310	1995–2019	WAPDA
11	Dainyor	74.37	35.93	1550	1997–2019	WAPDA
12	Deosai	75.54	35.09	4240	1995–2019	WAPDA
13	Hushe	76.37	35.42	3245	1995–2019	WAPDA
14	Khot Pass	72.58	36.52	3455	1995–2019	WAPDA
15	Khunjrab	75.42	36.84	4730	1995–2019	WAPDA
16	Naltar	74.18	36.17	3075	1995–2019	WAPDA
17	Ramma	74.81	35.36	3344	1995–2019	WAPDA
18	Rattu	74.80	35.15	2920	1995–2019	WAPDA
19	Shendoor	72.55	36.09	3560	1995–2019	WAPDA
20	Shigar	75.53	35.63	2560	1996–2019	WAPDA
21	Ushkor	73.39	36.05	2970	1995–2019	WAPDA
22	Yasin	73.50	36.40	3150	1995–2019	WAPDA
23	Zani	72.17	36.33	3000	1995–2013	WAPDA
24	Ziarat	74.46	36.77	3669	1995–2019	WAPDA

Table1 Detail of gauging stations in UIB

models have been selected based on the literature review and data availability (Ahmad & Rasul, 2018; Hasson, 2016; Shah et al., 2020). The CORDEX (coordinated regional downscaling experiment) project was initiated by the WCRP (World Climate Research Program) to provide reliable predictions of future climate change at the regional scale. The climatic factors selected for this study are maximum temperature, minimum temperature, average temperature, and precipitation. Details have been provided in Table 2. The data was downloaded using the WGET script in Linux, and data for the area of interest was extracted using coding in R software.

The data from 1976 to 2005 (the 1990s) from the RCM historical simulation period has been selected as the control period required to calculate change factors. The control period is selected that is representative of the long-term climate conditions of the study area. It should be long enough to capture the interannual and decadal variability of the climate in the region, typically spanning at least 30 years. The data for future simulation has been divided into two periods. The first future period for the mid-century is taken from 2041 to 2070 (considered 2050s later in this study), and the second future period for the end-century is considered from 2071 to 2100 (considered as 2080s later in this study). Both the future periods are taken for two emission scenarios: representative concentration pathways 4.5 (also known as RCP 4.5) and representative concentration pathways 8.5 (also known as RCP 8.5). RCP 4.5 is a stabilizing scenario in which the use of technologies to reduce greenhouse gases stabilizes the radiative forcing to 4.5 watts/m^2 at the end of this century. At the same time, RCP 8.5 is considered a high-risk scenario where the radiative forcing level will be 8.5 watts/m^2 by the end of this

century because of the absence of mitigation policies against greenhouse gas emissions.

Downscaling using LARS-WG6

Several studies have pointed out that precipitation and other climatic variables in the HKH region exhibit significant changes over short distances and considerable vertical gradients (Dahri et al., 2016; Wake, 1989). Moreover, the outputs from the RCMs remain prone to biases (Ehret et al., 2012; Tangang et al., 2020). Such systematic biases in GCMs and RCMs limit their direct use in regional climate change impact studies (Harding et al., 2014; Sunyer et al., 2012). Therefore, the gridded RCMs for the study area were downscaled to the station level for further use in impact studies. The downscaling for the current study was performed with the help of the sixth version of the Long Ashton Research Station Weather Generator (LARS-WG6). It is an inexpensive stochastic weather generator tool implemented by Semenov et al. (2002) for statistical downscaling of global or regional climate data to a local scale for impact assessment study of future climate at a daily timestep. The software can be accessed without any cost from https://sites.google.com/view/LARS-WG6/. The capability of LARS-WG6 for downscaling climatic parameters, including temperature and precipitation, has been ascertained in diverse climates worldwide.

The first step of model calibration involves the analysis of observed data using the "Site Analysis" option and determining their statistical properties. LARS-WG6 generates synthetic weather data with the same statistical properties as observed data but differing on a day-to-day basis (Semenov et al., 2002). The second stage of model validation involves comparing the statistical properties of synthetic data

Table 2 Detail of RCMs used in the study

Sr. No	RCM	Driving GCM	Short name (adopted in this study)	Historical simulation period	Future simulation period	Scenario	Horizontal resolution
1	REMO 2009	MPI-M-MPI-ESM-LR	REMO	1961–2005	2006–2100	RCP4.5, RCP8.5	0.44°
2	RCA4	ICHEC-EC-EARTH	ICHEC	1951–2005	2006–2100	RCP4.5, RCP8.5	0.44°
3	RCA4	IPSL-IPSL-CM5A-MR	IPSL	1951–2005	2006–2100	RCP4.5, RCP8.5	0.44°
4	RCA4	MPI-M-MPI-ESM-LR	MPI	1951–2005	2006–2100	RCP4.5, RCP8.5	0.44°
5	RCA4	NCC-NorESM1-M	NOR	1951–2005	2006–2100	RCP4.5, RCP8.5	0.44°
6	RCA4	NOAA-GFDL-GFDL-ESM2M	NOA	1951–2005	2006–2100	RCP4.5, RCP8.5	0.44°

with observed data (Chen et al., 2013; Fenta Mekonnen & Disse, 2018; Kavwenje et al., 2022). Statistical tests for model validation include comparing the probability distribution, variance, and means with the help of the Kolmogorov–Smirnov (KS) test, *F*-test, and *t*-test, respectively. The last step involves the creation of a scenario file using the RCMs data and generating future output at the local scale. The model can use only 1 year of data to generate synthetic climate data. However, it is recommended to use at least 20–30 years of data to better represent the climate for the site under consideration (Semenov et al., 2002)—the use of long time series aids in capturing less frequent or extreme climate events.

Scenario files were created to generate future climate time series for a station by calculating change factors. These change factors were computed on a monthly scale by calculating the differences between the data of the control period and future periods of six different RCMs mentioned in the data section for the two different emission scenarios. These change factors were then applied to LARS-WG6 parameters, and hence, a local-scale future simulation was generated for the required number of years at a daily time step. Figure 2 represents a flow chart of LARS-WG6 working.

Results and discussions

Calibration and validation of LARS-WG6

The capability of LARS-WG6 was evaluated by computing the statistical properties of the observed time series and then comparing these with the synthetic time series. This calibration and validation process was executed for each of the UIB's twenty-four meteorological stations to assess the performance of LARS-WG6 for downscaling RCMs.

The Kolmogorov–Smirnov (KS) test is executed to check the goodness of fit of the seasonal distributions of dry and wet (DW) series, distributions of daily precipitation (D.pr), as well as distributions of daily maximum (D.T$_{max}$) and daily minimum (D.T$_{min}$) temperature. The second test is the *F*-test which is conducted to check monthly precipitation variances (MV. pr). In contrast, the third test, i.e., the *t*-test, is carried out to validate the likeness of monthly average precipitation (MM.pr), a monthly average of daily maximum temperature (DM.T$_{max}$), and a monthly

average of daily minimum temperature (DM.T$_{min}$). All the tests mentioned above calculate a *p*-value. The *p*-value accepts or rejects the hypotheses that the observed and generated data may belong to the same distribution at the 5% significance level.

Table 3 shows the results for assessing the performance of LARS-WG6 for each of the twenty-four stations in UIB. The values in this table show how often the results differ significantly at a 5% significance level. The total number of tests performed is eight each for the dry and wet series and 12 for the remaining. The performance of LARS-WG6 is considered to be excellent if the values in the table approach zero. It is clear from the table that the Wet Series, Dry Series, D.pr, D.T$_{min}$, and D.T$_{max}$ do not differ significantly at all twenty-four stations; for MM.pr, MV.pr, DM.T$_{max}$, and DM.T$_{min}$, the average results were found to be 0.04, 3.96, 0.17, and 0.21, respectively. It is therefore concluded that LARS-WG6 is capable of modeling the distributions and means of this study's three climatic variables for all the months as compared to the monthly variances of precipitation (MV.pr).

Figure 3 compares the observed mean monthly precipitation (pr) along with the maximum and minimum temperature (T$_{max}$ and T$_{min}$) with the simulated time series for each of the twenty-four gauging stations. The graphical results for precipitation show satisfactory results where the simulated mean monthly precipitation matched well with the observed data for all stations. Similarly, in the case of maximum and minimum temperature, the simulated values perfectly matched the observed values for all the stations.

Figure 4 compares observed and simulated data for all 24 meteorological stations with the help of the Taylor diagram. A Taylor diagram represents how well a numerical model or simulation matches observed data (Taylor, 2001). It is visible that the data simulated by LARS-WG6 is in good agreement with the observed data having a strong correlation varying from 0.86 to 0.99.

The daily time series generated by LARS-WG6 has been calibrated for 1995–2005 and validated for 2010–2019. The calibration results are shown in Fig. 8, and validation results are shown in Fig. 9 in Appendix-A using the box and whisker plots. The plots show the distribution of observed daily data and generated daily data for all three variables for each of the twenty-four stations. These plots provide clear information about the range and variability of the daily data. The distribution of the simulated
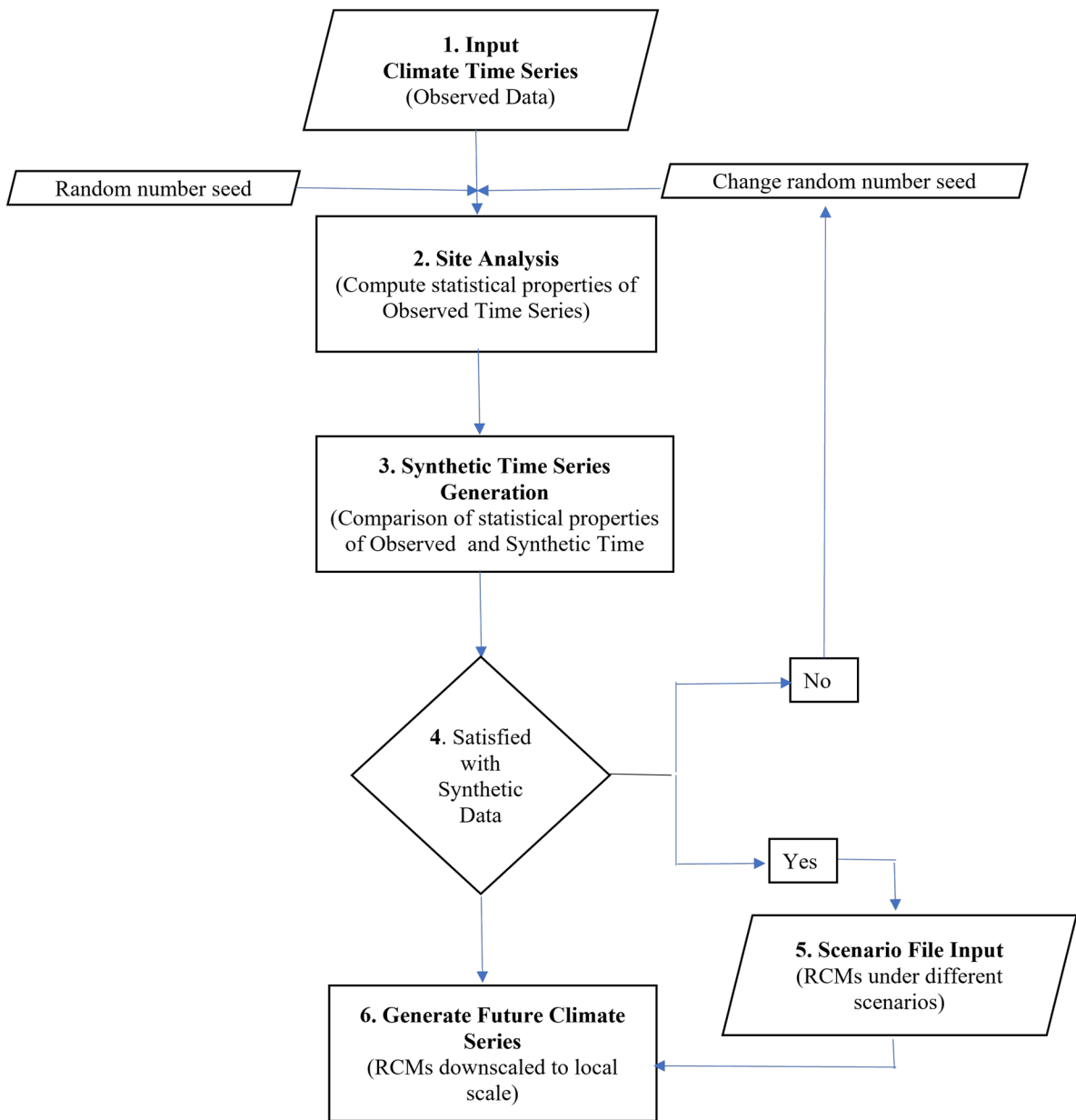
```
┌────────────────────────────┐
│      1. Input              │
│  Climate Time Series       │
│     (Observed Data)        │
└────────────────────────────┘
```

**1. Input
Climate Time Series**
(Observed Data)

Random number seed → ← Change random number seed

2. Site Analysis
(Compute statistical properties of
Observed Time Series)

**3. Synthetic Time Series
Generation**
(Comparison of statistical properties
of Observed and Synthetic Time

4. Satisfied
with
Synthetic
Data

No

Yes

5. Scenario File Input
(RCMs under different
scenarios)

**6. Generate Future Climate
Series**
(RCMs downscaled to local
scale)

Fig. 2 Flow chart of LARS-WG6

data, as represented by the box and whisker plot, is comparable to that of the observed data, with no significant differences in the central tendency or spread of values. Therefore, based on these statistical and graphical results, it is inferred that the LARS-WG6 is a trustable tool for future projections of temperature and precipitation predictions in UIB.

Downscaling with LARS-WG6

As the LARS-WG6 model has been found suitable during the performance evaluation phase, the climate scenarios can be downscaled from six selected RCMs under RCP 4.5 and RCP 8.5 for the two defined future periods.

Table 3 Results of LARS-WG6 performance evaluation

Variable	D.pr	MM.pr	MV.pr	D.T_{min}	DM.T_{min}	D.T_{max}	DM.T_{max}	Wet series	Dry series
Station /Test	KS test	T-test	F-test	KS-test	T-test	KS-test	T-test	KS-test	KS-test
ASTORE	0	1	3	0	0	0	0	0	0
BUNJI	0	0	3	0	0	0	0	0	0
BURZIL	0	0	3	0	1	0	0	0	0
CHILLAS	0	0	2	0	1	0	0	0	0
CHITRAL	0	0	2	0	0	0	0	0	0
DAINYOR	0	0	4	0	0	0	1	0	0
DEOSAI	0	0	4	0	0	0	0	0	0
DIR	0	0	3	0	0	0	0	0	0
DROSH	0	0	1	0	0	0	0	0	0
GILGIT	0	0	4	0	0	0	0	0	0
GUPIS	0	0	5	0	0	0	0	0	0
HUSHE	0	0	5	0	1	0	0	0	0
KHOTPAS	0	0	4	0	1	0	0	0	0
KHUNJRAB	0	0	4	0	1	0	0	0	0
NALTAR	0	0	4	0	0	0	0	0	0
RAMA	0	0	4	0	0	0	0	0	0
RATTU	0	0	3	0	0	0	2	0	0
SHENDUR	0	0	4	0	0	0	0	0	0
SHIGAR	0	0	3	0	0	0	1	0	0
SKARDU	0	0	4	0	0	0	0	0	0
USHKOR	0	0	4	0	0	0	0	0	0
YASIN	0	0	4	0	0	0	0	0	0
ZANI	0	0	4	0	0	0	0	0	0
ZIARAT	0	0	4	0	0	0	0	0	0
AVERAGE	0	0.04	3.54	0	0.21	0	0.17	0	0
TOTAL NO. OF TESTS	12	12	12	12	12	12	12	8	8

Downscaling of maximum temperature (T_{max})

Figure 5 presents the projections of annual average T_{max} by the six RCMs under two emission scenarios in two future periods. Results represent an increase in T_{max} for all RCMs and both RCPs during both the mid-century and end-century periods for all 24 stations. It is also apparent that the extent of variation in T_{max} is higher in the end-century than in the mid-century for all RCMs under both emission scenarios. Moreover, the increase in T_{max} is the lowest under RCP 4.5 during the mid-century (0.87 °C for Hushe to 1.97 °C for Chillas) predicted by REMO and largest under RCP 8.5 during the end-century (7.51 °C for Ziarat to 10.14 °C for Gupis) predicted by IPSL, respectively. Among all RCMs and stations,

the IPSL simulation scenarios consistently provided the highest rise in future predictions under RCPs for both periods. Considering the average ensemble values, the increase in T_{max} varies from 1.58 °C for Rattu and Hushe to 3.08 °C for Bunji under RCP4.5 2050, 2.35° for Rattu to 3.49 °C for Drosh under RCP 4.5 2080, 2.38 °C for Rattu to 3.85 °C for Drosh under RCP 8.5 2050, and 4.82 °C for Shigar to 6.45 °C for Drosh under RCP 8.5 2080. Figure 6 shows the spatial variation of T_{max} over UIB. The average value of the multi-model ensemble indicates an increase of 2.04 °C and 2.82 °C under RCP 4.5 for the 2050s and 2080s, respectively. Similarly, the ensemble predicted an increase of 2.96 °C and 5.58 °C under RCP 8.5 for the 2050s and 2080s, respectively. This indicates that UIB is expected to get warmer in the future.
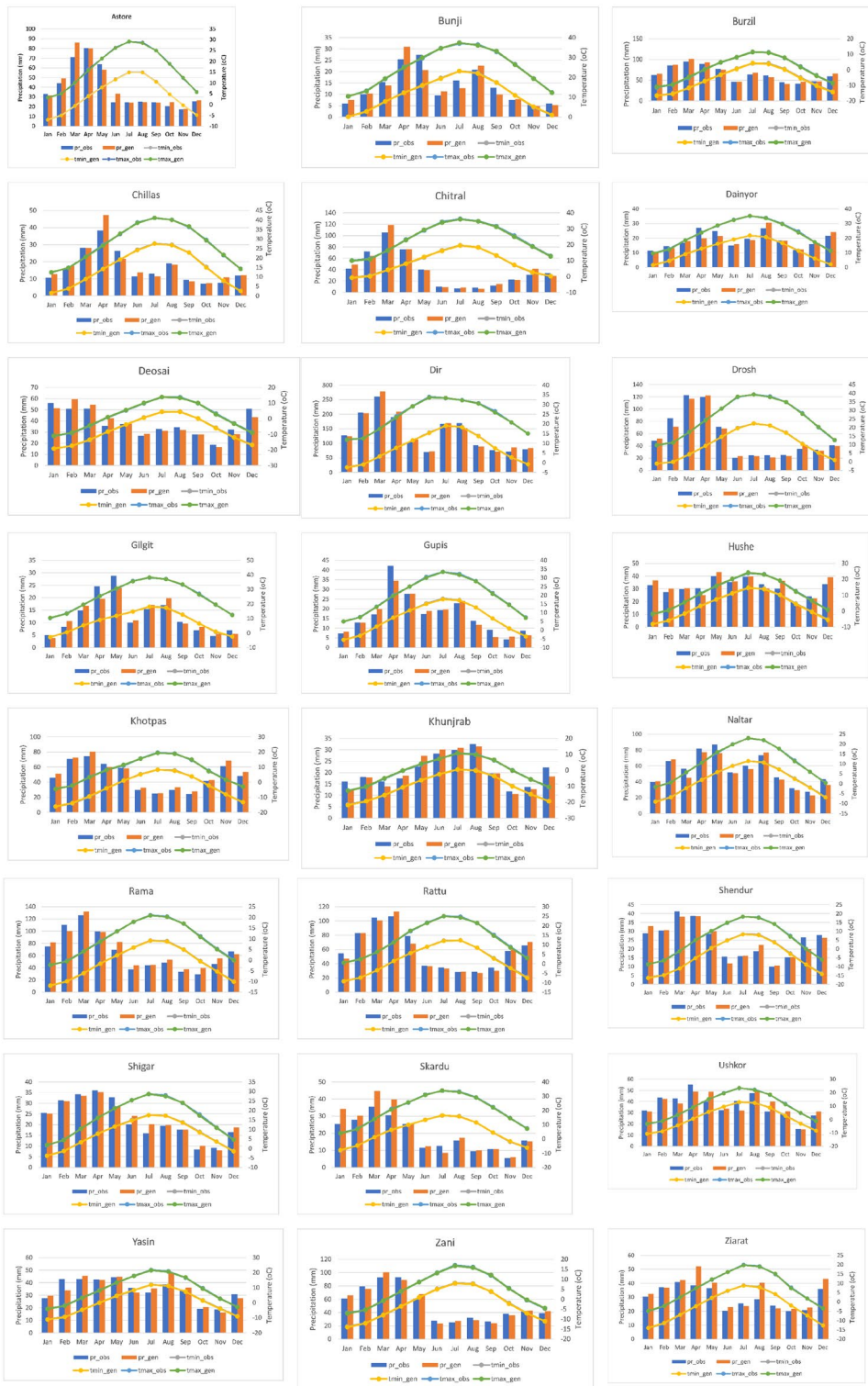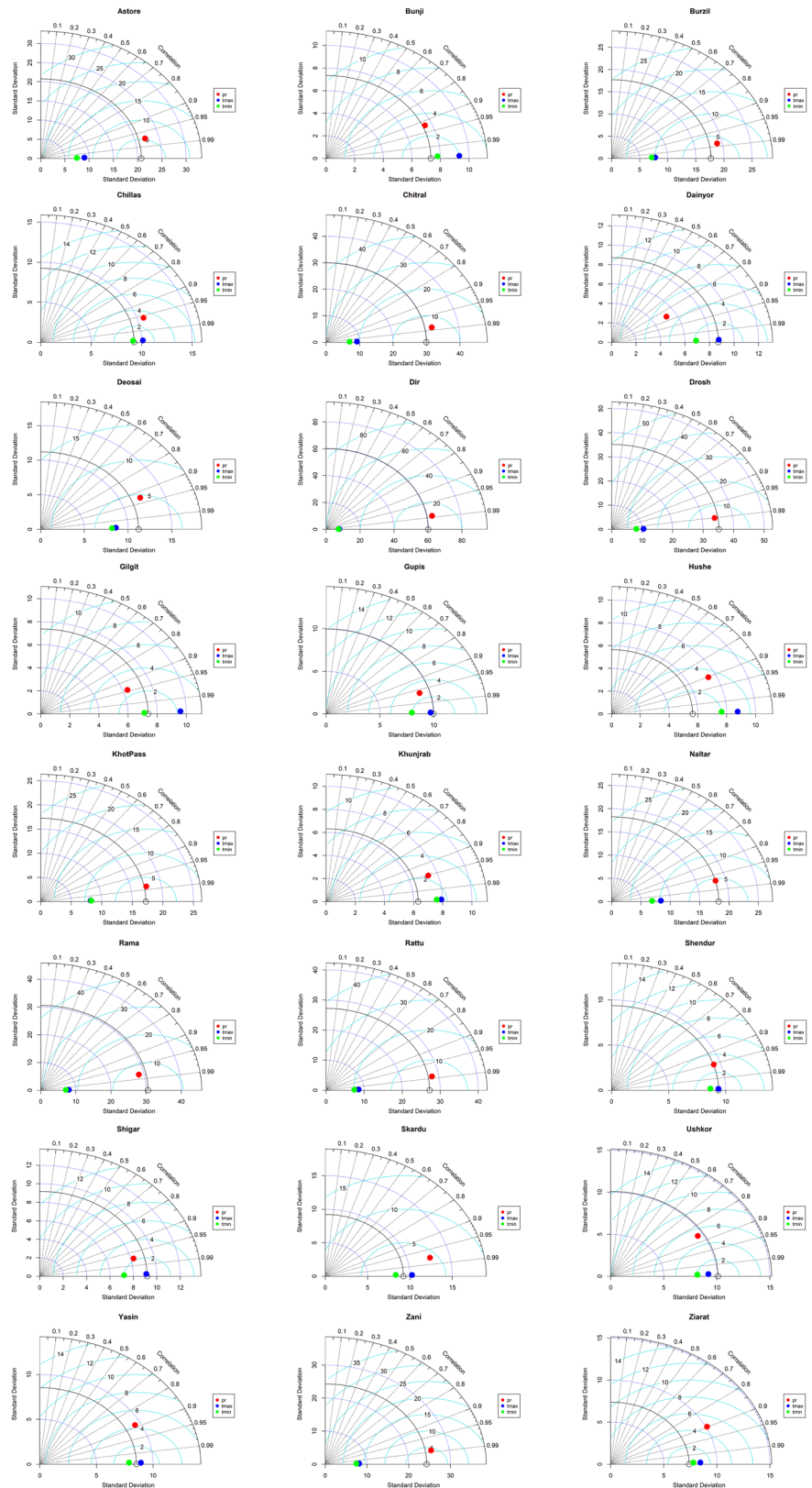
Fig. 3 Comparison of observed and generated mean monthly T_{max}, T_{min}, and precipitation for 24 stations of the study area

Fig. 4 Taylor diagram for comparison of observed and generated T$_{max}$, T$_{min}$, and precipitation for 24 stations of the study area
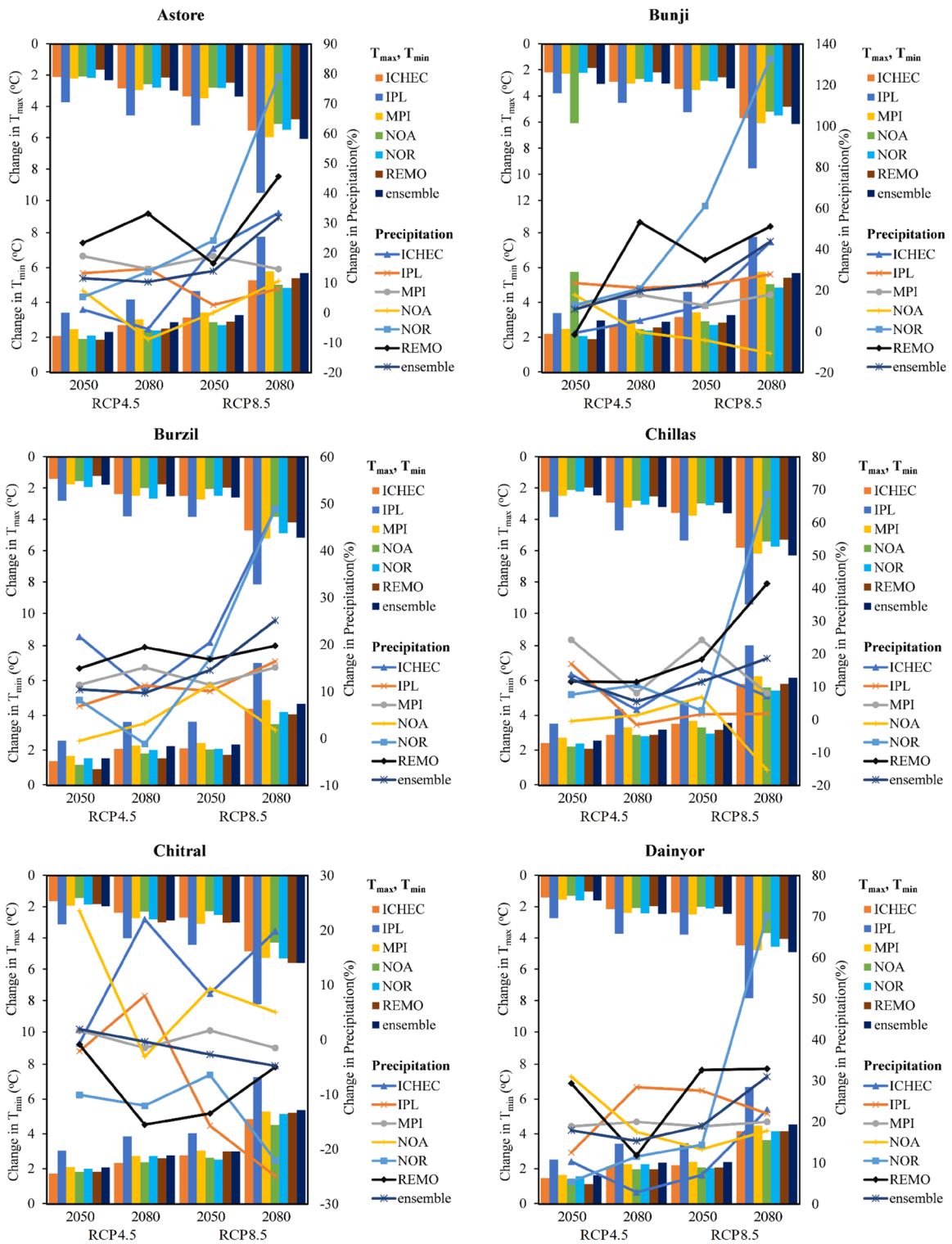
Fig. 5 Changes in average annual T$_{max}$, T$_{min}$, and precipitation for six RCMS for 24 stations for 2050 and 2080 under RCP 4.5 and RCP 8.5
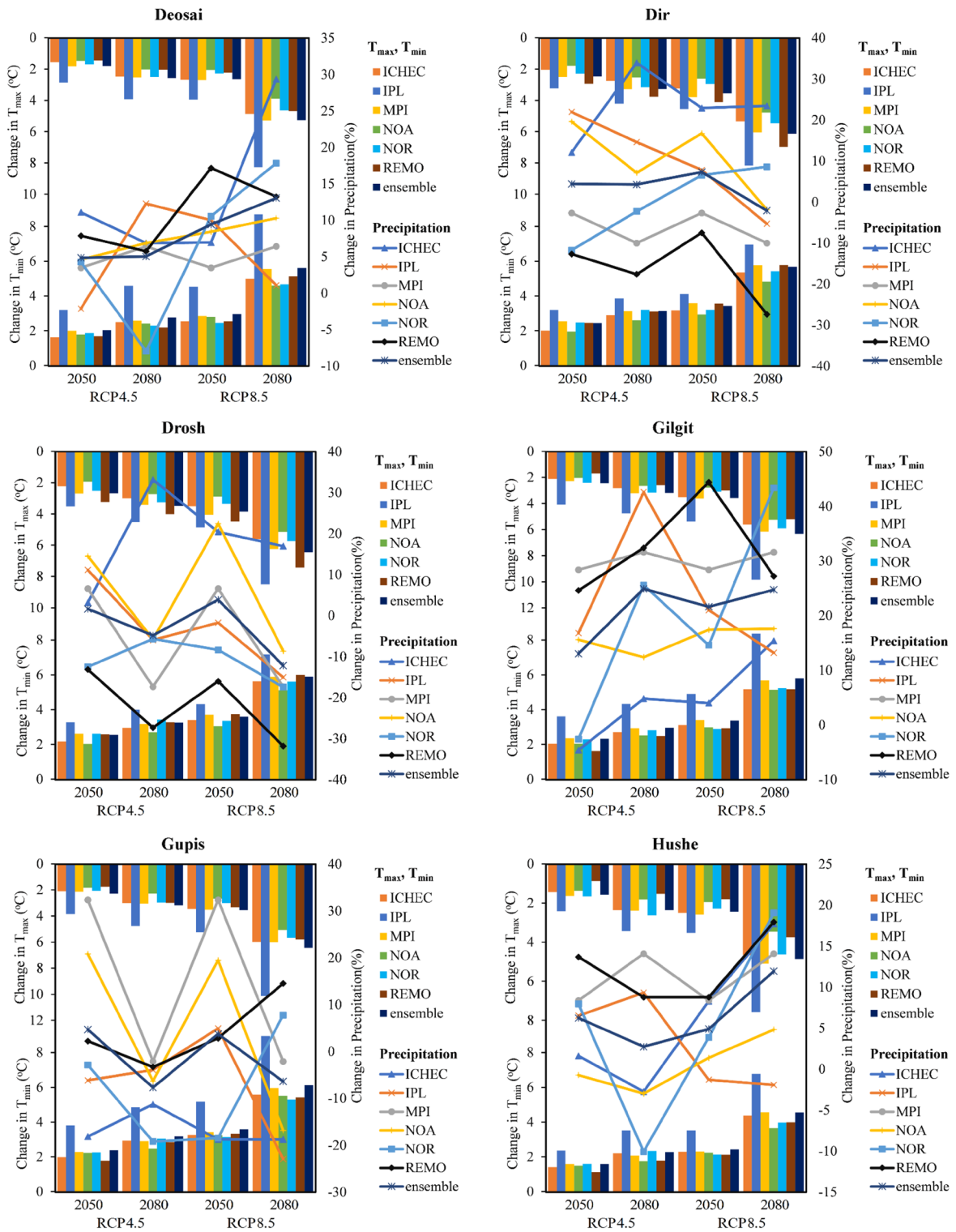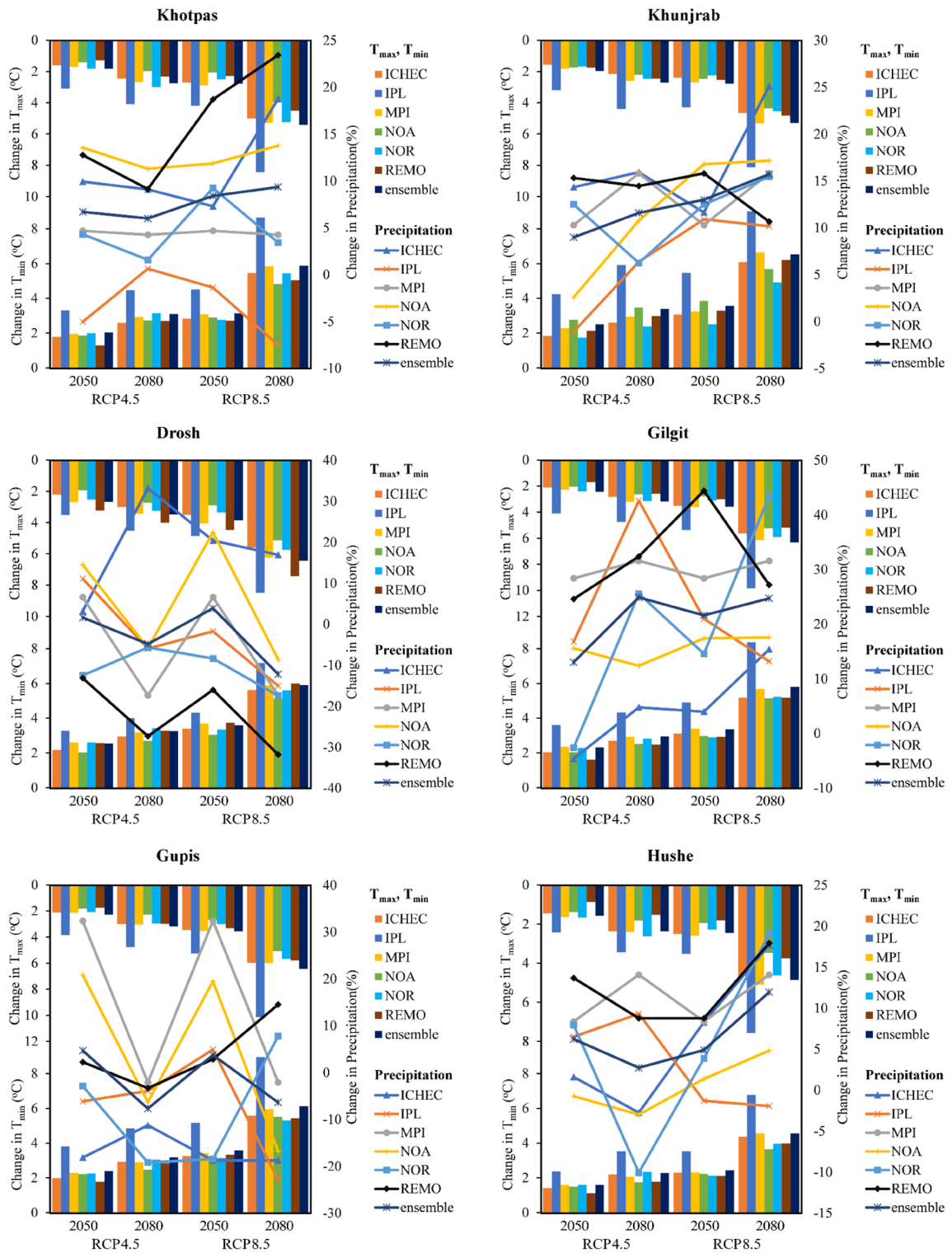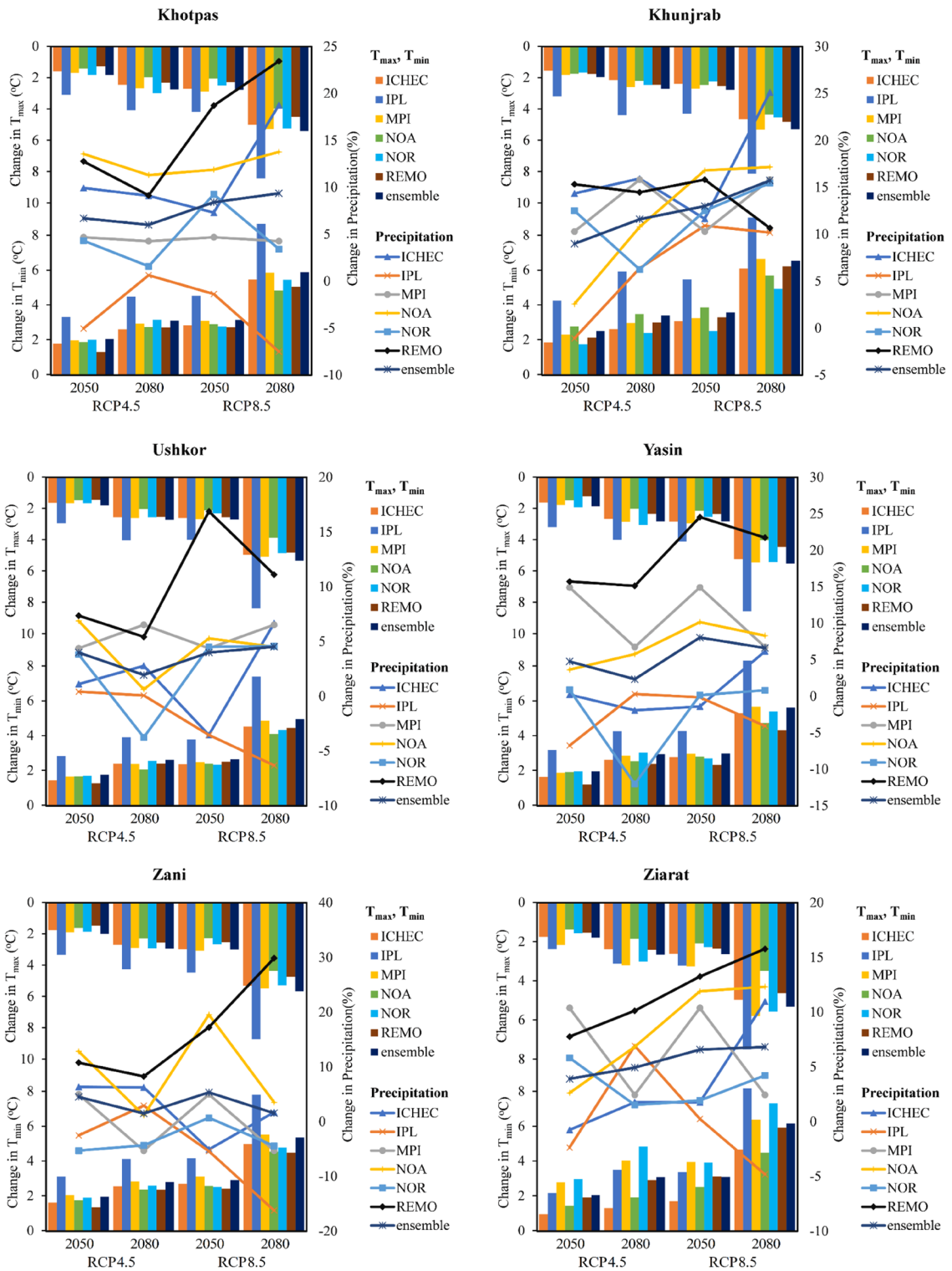
Fig. 5 (continued)

Fig. 5 (continued)

Fig. 5 (continued)
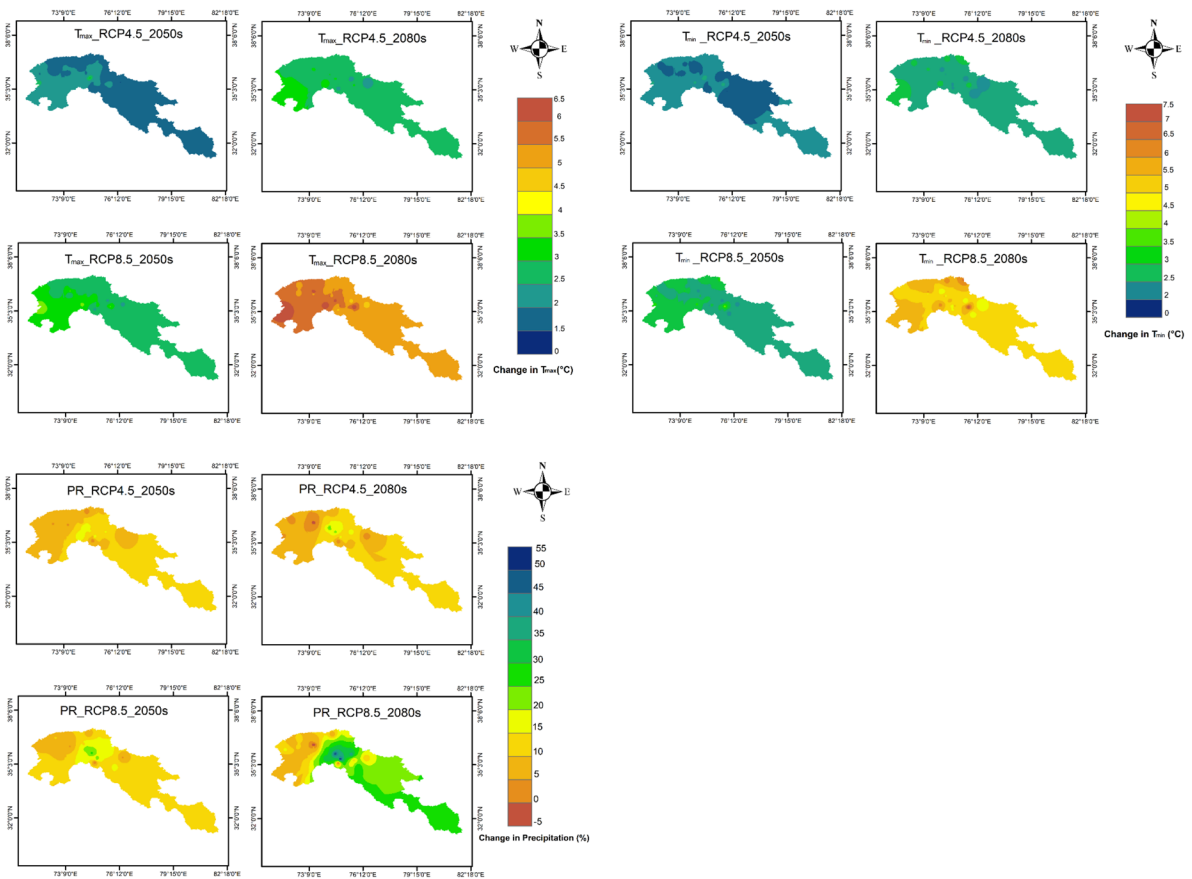
Fig. 6 Changes in annual T_{max}, T_{min}, and precipitation projected by the multi-model ensemble for 2050 and 2080 under RCP 4.5 and RCP 8.5

The projected increase in maximum temperature in the UIB requires extreme attention as it may cause water stress, mainly if there is a reduction in precipitation in the basin.

Downscaling of minimum temperature (T_{min})

Figure 5 depicts the variations in annual average T_{min} projected by six RCMs under RCP 4.5 and RCP 8.5 in two future periods. Results for each of the 24 sites exhibit the same trend toward higher values as T_{max}. It was also noticed that for all four scenarios, projections under RCP 4.5 in the mid-century consistently showed the smallest increase in T_{min} (0.81 °C for Shigar, predicted by REMO, to 2.3 °C for Skardu, predicted by ICHEC). In contrast, those under RCP8.5 in the end-century consistently

showed the most significant increase (6.33 °C for Rama to 10.65 °C for Skardu) predicted by IPSL. Like T_{max}, among all the RCMs, the IPSL simulations always depict the most significant increment in future projections under both RCPs. The average ensemble of multiple RCMs shows an increase of T_{min} from 1.53 °C for Burzil to 2.95 °C for Bunji during RCP 4.5 2050s and 4.54 °C for Dainyor to 7.04 °C for Skardu during RCP 8.5 2080s. The average annual increase in T_{min} over UIB is predicted to be 2.07 °C and 2.80 °C for RCP 4.5 during the 2050s and 3.00 °C and 5.47 °C for RCP 8.5 during the 2080s.

The T_{max} and T_{min} results indicate that the Upper Indus Basin's future climate will likely be warmer. However, the RCMs disagree on the magnitude of variation over the two future periods. This study's findings agree with the IPCC 5th assessment report

and confirm that RCP8.5 projections are higher than RCP4.5, which may be attributed to the former's limited mitigation and adaptation policies. The temperature trends expected by different RCMs are also consistent with previous research findings by Stott and Kettleborough (2002), Fenta Mekonnen and Disse (2018), and Kavwenje et al. (2022) where they all noticed that the increment in temperature was more sensitive to emission scenario in the 2080s as compared to 2050s. Akhtar et al. (2008) used PRECIS Regional Climate Model and predicted that temperature would show increasing trends towards the end of this century. Ismail et al. (2020) have used an ensemble of four GCMs to predict the future climate over UIB. The ensemble projects an increase of 6 °C in temperature under the RCP 8.5 scenario by the end of this century. These studies agree with our findings, where an average increase of 5.47 °C in T_{min} and 5.58 °C in T_{max} is projected over UIB by the end of the century under RCP 8.5.

In general, based on the projected temperature trends under various climate change scenarios, it is clear that throughout this century, the UIB will experience pronounced warming trends which could directly impact the availability of water resources.

The seasonal variation of T_{min} and T_{max} is shown in Fig. 7. The highest increase in both T_{min} and T_{max} is observed in winter and autumn under RCP 8.5 by the end of the century, whereas the summer season exhibits the lowest increase in temperature as compared to the rest of the months. A high winter warming over the UIB aligns with earlier studies (Ali et al., 2015; Almazroui et al., 2020). The lesser increase in temperature during summer may be governed by a combination of factors, including increased monsoon precipitation, decreased solar radiation (Bashir et al., 2017), the impact of large-scale circulations (Fowler & Archer, 2006), and dynamics related to regional snow (Kumar et al., 2019).

The overall projected increase in temperature has significant implications for the basin, particularly in terms of water stress. Higher temperatures can lead to increased evapotranspiration and water loss from the basin, and coupled with a reduction in precipitation, this can cause water stress in the region. This has implications for agriculture, where higher temperatures and water stress can lead to decreased crop yields and a shift in cropping patterns. Additionally, increased temperatures can also impact the snowpack in the region, leading to changes in the timing and amount of snowmelt runoff, affecting water availability in the basin. Therefore, it is essential to carefully consider the potential impacts of increased temperature in the UIB and develop strategies to mitigate the adverse effects of temperature rise. This may involve implementing measures to conserve water resources, such as improving irrigation efficiency and reducing wastage, promoting drought-resistant crops, and introducing better water management practices. It is also crucial to continue monitoring the basin's temperature and precipitation patterns and refine projections to better understand and plan for the future impacts of climate change on the region.

Downscaling of precipitation (pr)

The percent change in average annual precipitation envisaged by the six RCMs and their ensemble average under the two emission scenarios for mid-century and end-century in the UIB is depicted in Fig. 5. It is clear from these graphs that the change in precipitation has no discernible trend for the future time slices for all the six RCMs under both emission scenarios. In the future, both increases and decreases have been predicted in the average annual precipitation for the twenty-four meteorological stations. The non-uniform behavior of precipitation under various scenarios and periods, as investigated in this study, is in agreement with the findings of Agarwal et al. (2014) in Nepal, Fenta Mekonnen and Disse (2018) in the Nile, Kavwenje et al. (2022) in Malawi, and Alotaibi et al. (2018) in Saudi Arabia. Therefore, evaluating the impact of a broad range of precipitation projections during the twenty-first century may yield a range of reasonable variations in future runoff quantities in the basin. However, it is also observed in the current study that most RCMs depict an increase rather than a decrease in most stations for all future scenarios. Out of 24, twenty stations show
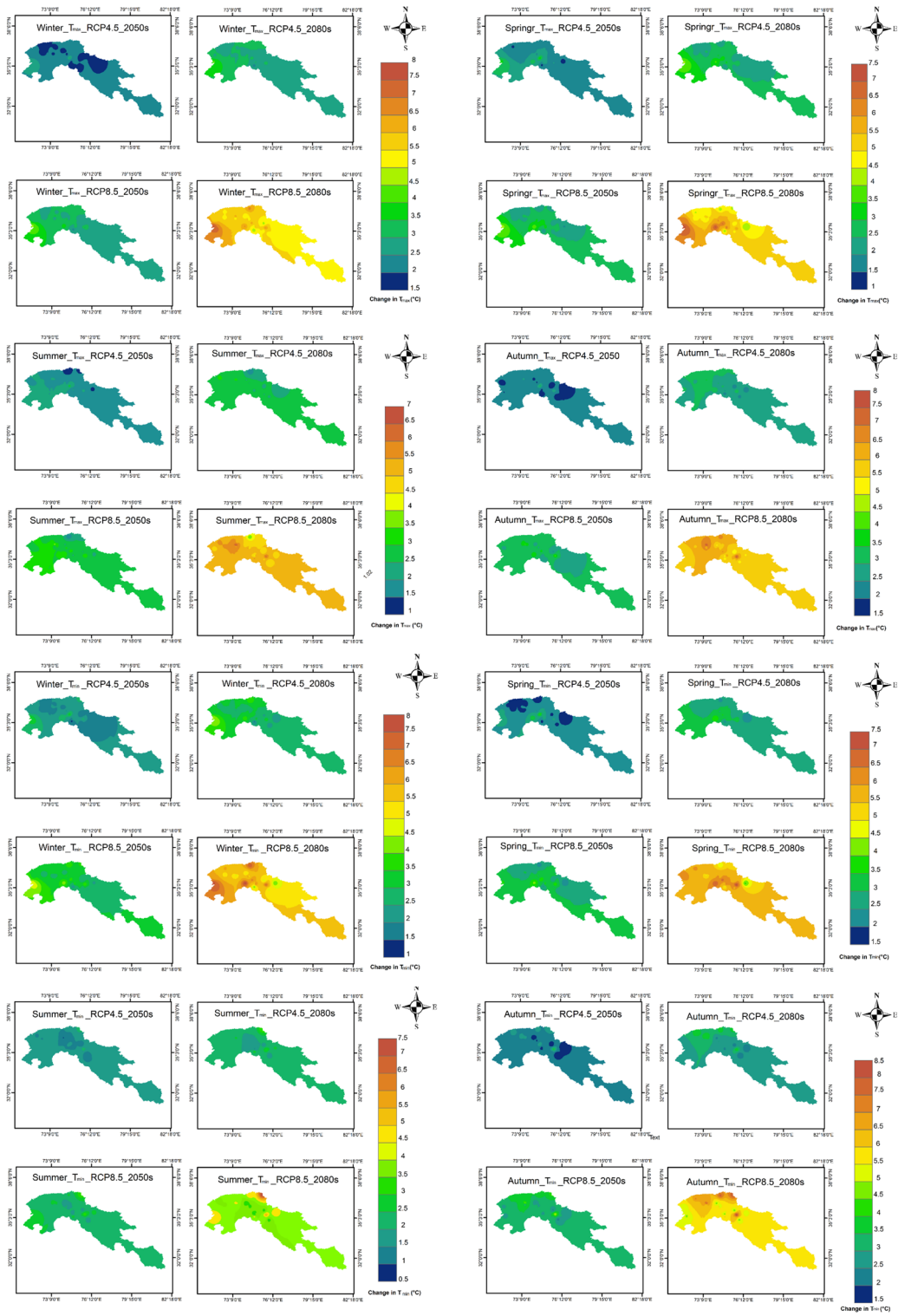
Fig. 7 Changes in seasonal T$_{max}$, T$_{min}$, and precipitation projected by the multi-model ensemble for 2050 and 2080 under RCP 4.5 and RCP 8.5

increasing precipitation. The multi-model ensemble predicts an average increase of 9.66% and 9.27% in precipitation over the entire basin under RCP 4.5 for the 2050s and 2080s, respectively.

Similarly, under RCP 8.5, the predicted increase in precipitation by the ensemble is 12.71% and 18.56% for the 2050s and 2080s, respectively. These agree with the predictions (Ismail et al., 2020). According to them, the average annual precipitation increases by 2–6% under RCP 2.6 and 6–15% under RCP 8.5. Similarly, Forsythe et al. (2014) have predicted an increase of 18% over UIB using a stochastic rainfall model. The spatial pattern of annual precipitation by the ensemble is shown in Fig. 6. Precipitation is increasing from west to east. A similar spatial pattern has been observed by Pomee and Hertig (2022). This can be attributed to the strong effect of the westerly system on

the West of UIB and the monsoon-dominant influence towards the eastern side of UIB (Bookhagen & Burbank, 2010; Maussion et al., 2014).

Future increases in precipitation may present a favorable chance for farmers who practice rainfed agriculture to increase crop yields and alter their way of life. However, it is essential to recognize that the predicted increase in precipitation may also result in new challenges, such as an increased risk of flooding and soil erosion. The seasonal variation of precipitation over UIB is shown in Fig. 7. The highest increase in precipitation is found during the summer months, with the highest increase under the RCP 8.5 scenario by the end of the century. Our finding of increased precipitation in summer months aligns with those of Lutz et al., (2016a2016b).
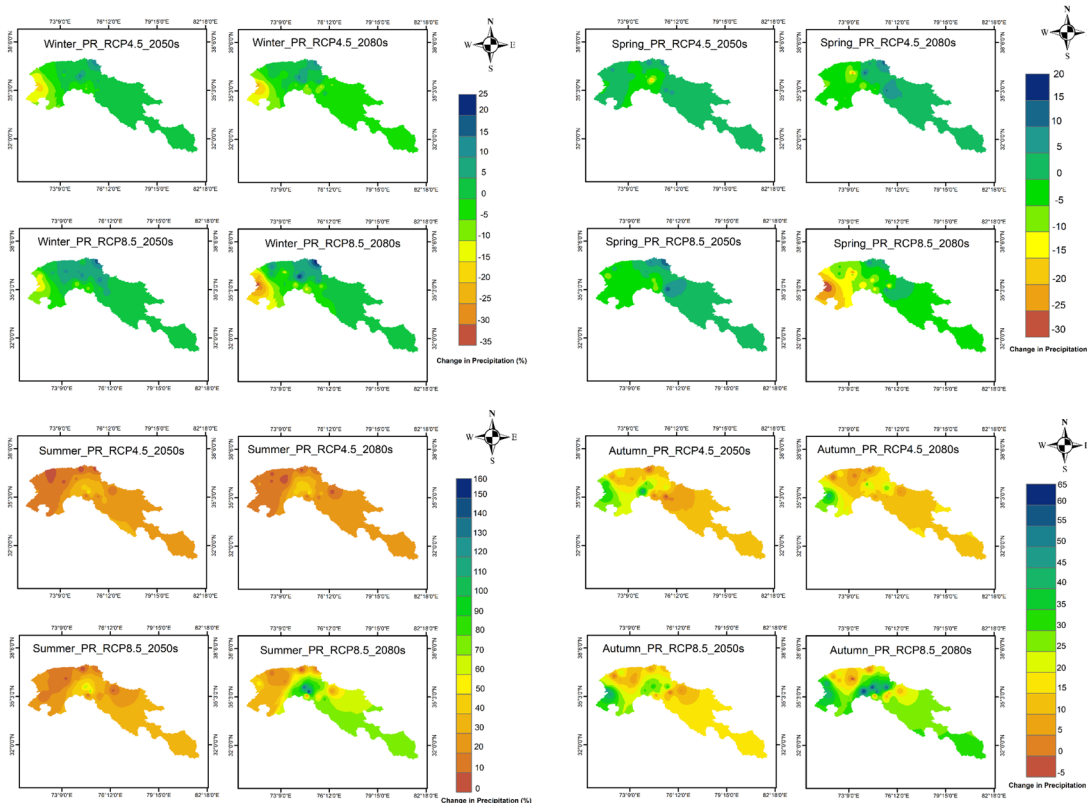

Fig. 7 (continued)

Similarly, a 20–40% increase in summer precipitation predicted by Kulkarni et al. (2013) over HKH is in line with our finding of 21.84% and 22.73% increases in summer precipitation under RCP 4.5 for the 2050s and 2080s, respectively, and 27.42% and 54.99% increases in summer precipitation under RCP 8.5 for the 2050s and 2080s respectively. Relatively no change to a reduction in precipitation is projected in the winter and spring seasons, with a severe reduction on the western side during RCP 8.5 by the end of the century. The results are in line with Palazzi et al. (2015). Increased summer precipitation could lead to higher river discharge in the UIB during the summer. This could result in flooding and increased erosion along the riverbanks. The increased summer precipitation could also increase the recharge of groundwater aquifers in the region. This could increase water availability for agriculture and other uses during the dry season. However, no significant change in winter precipitation could lead to reduced snow accumulation in the winter, which could have implications for water availability during the summer. Snowmelt provides an essential water source for the region, and reduced snow accumulation could decrease river discharge during the summer. It is, therefore, crucial to evaluate the potential impacts of a range of precipitation projections on the basin's runoff quantities and consider adaptive strategies to mitigate any negative impacts.

Conclusion

In the present research, the model performance of LARS-WG6 to downscale daily time series of precipitation (pr) and maximum (T_{max}) and minimum (T_{min}) temperatures in the Upper Indus Basin was evaluated. After getting satisfactory results from statistical and graphical comparison, LARS-WG6 was then used to project future changes for three climatic variables, i.e., pr, T_{min}, and T_{max} for

twenty-four stations in UIB from the outputs of six RCM and their ensemble under the RCP 4.5 and RCP 8.5 scenario for the periods of 2041–2070 and 2071–2100. From this research, it is deduced that the LARS-WG6 tool is capable of downscaling daily precipitation and daily maximum and minimum temperatures for UIB. The downscaled precipitation projected by six RCMs and their ensemble under the two emission scenarios for two future periods has inconsistent changing trends. However, overall, an increase in precipitation is projected by most of the stations. On the other hand, the downscaled projections of T_{max} and T_{min} from all six RCMs and their ensemble exhibited a continuous and similar increasing trend in future periods under both RCP 4.5 and RCP scenarios 8.5 in the whole UIB.

Declarations

All authors have read, understood, and have complied as applicable with the statement on "Ethical responsibilities of Authors" as found in the Instructions for Authors and are aware that, with minor exceptions, no changes can be made to authorship once the paper is submitted.

Competing interests The authors declare no competing interests.

Appendix

Fig. 8 Box Plots for Comparison of Observed and Generated T_{max}, T_{min} and precipitation for 24 stations of the study area during Calibration Period
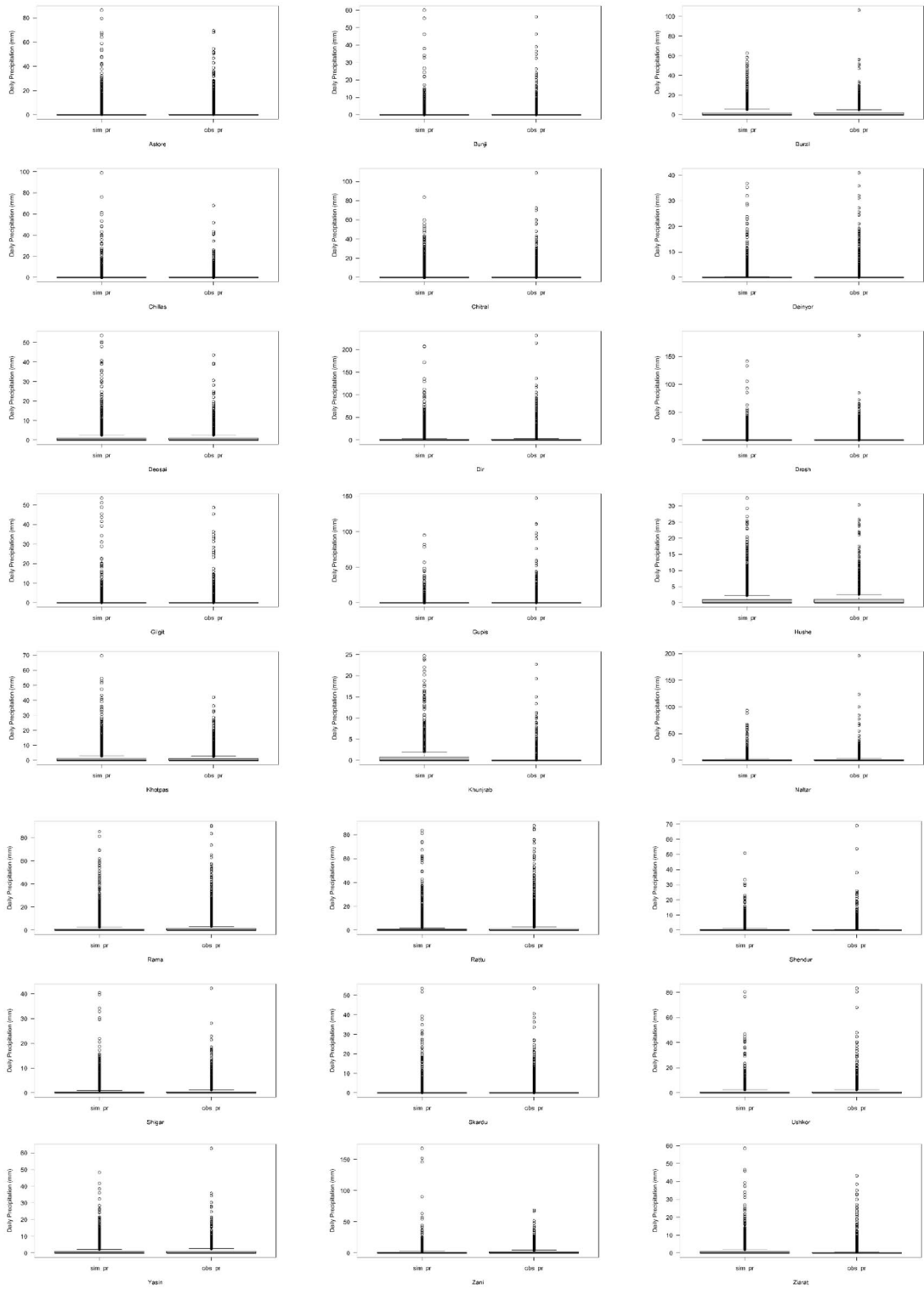
Fig. 8 (continued)

Fig. 9 Box Plots for Comparison of Observed and Generated T_{max}, T_{min} and precipitation for 24 stations of the study area during Validation Period
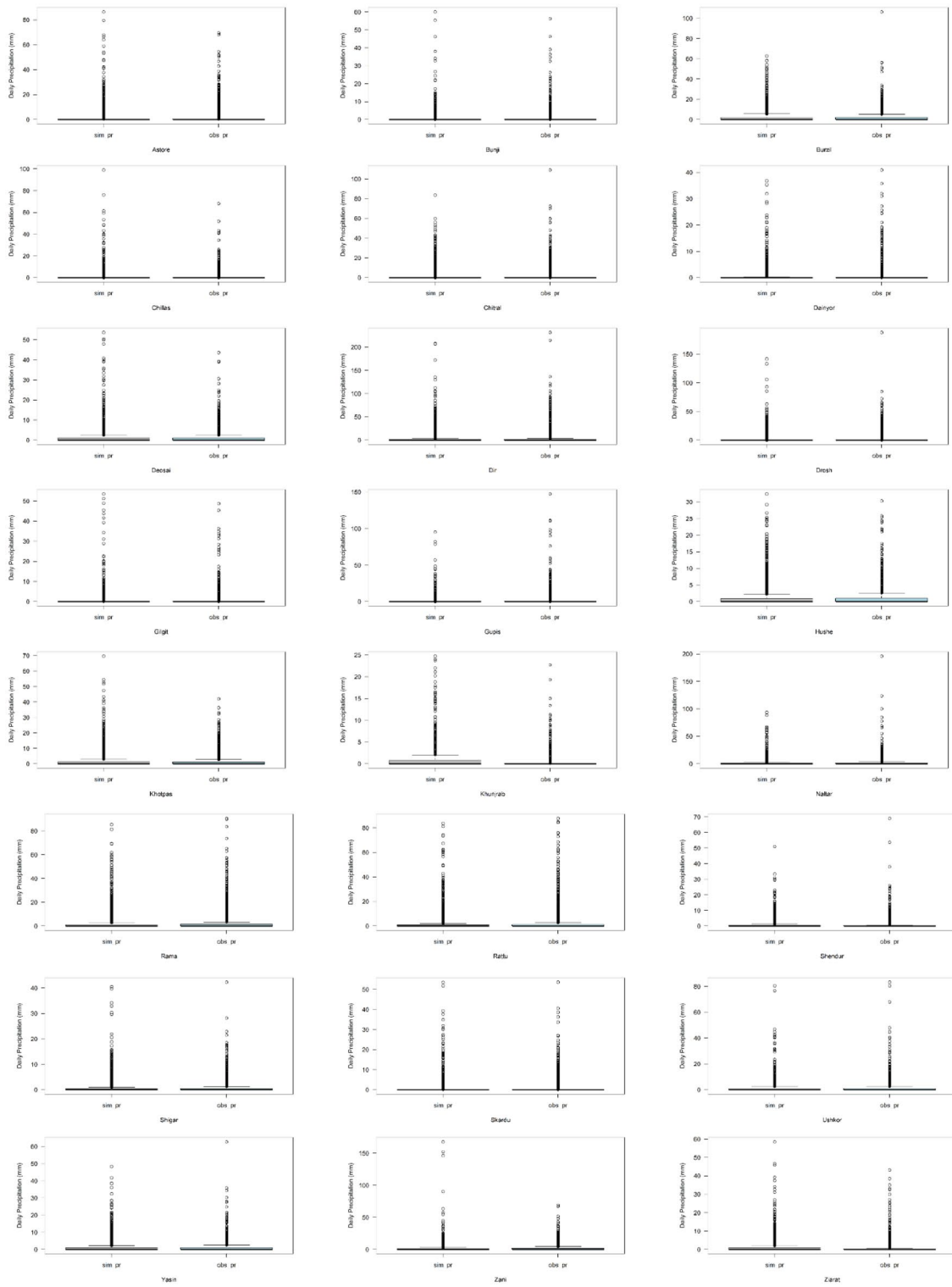
Fig. 9 (continued)

References

Abiodun, B. J., & Adedoyin, A. (2016). A modelling perspective of future climate change. In T. M. Letcher (Ed.), *Climate Change* (pp. 355–371). Elsevier.

Agarwal, A., Babel, M. S., & Maskey, S. (2014). Analysis of future precipitation in the Koshi river basin, Nepal. *Journal of Hydrology, 513*, 422–434.

Ahmad, B., & Rasul, G. (2018). Statistically downscaled projections of CORDEX South Asia using quantile mapping approach over Pakistan region. *International Journal of Global Warming, 16*(4), 435–460.

Akhtar, M., Ahmad, N., & Booij, M. J. (2008). The impact of climate change on the water resources of Hindukush–Karakorum–Himalaya region under different glacier coverage scenarios. *Journal of Hydrology, 355*(1), 148–163. https://doi.org/10.1016/j.jhydrol.2008.03.015

Ali, S., Li, D., Congbin, F., & Khan, F. (2015). Twenty first century climatic and hydrological changes over Upper Indus Basin of Himalayan region of Pakistan. *Environmental Research Letters, 10*(1), 014007.

Almazroui, M., Saeed, S., Saeed, F., Islam, M. N., & Ismail, M. (2020). Projections of precipitation and temperature over the South Asian countries in CMIP6. *Earth Systems and Environment, 4*, 297–320.

Alotaibi, K., Ghumman, A. R., Haider, H., Ghazaw, Y. M., & Shafiquzzaman, M. (2018). Future predictions of rainfall and temperature using GCM and ANN for arid regions: A case study for the Qassim Region, Saudi Arabia. *Water, 10*(9), 1260.

Baronetti, A., Dubreuil, V., Provenzale, A., & Fratianni, S. (2022). Future droughts in northern Italy: High-resolution projections using EURO-CORDEX and MED-CORDEX ensembles. *Climatic Change, 172*(3), 22. https://doi.org/10.1007/s10584-022-03370-7

Barros, V. R., Field, C. B., Dokken, D. J., Mastrandrea, M. D., Mach, K. J., Bilir, T. E., Chatterjee, M., Ebi, K. L., Estrada, Y. O., & Genova, R. C. (2014). Climate change 2014 impacts, adaptation, and vulnerability Part B: regional aspects: working group II contribution to the fifth assessment report of the intergovernmental panel on climate change. In *Climate Change 2014: Impacts, Adaptation and Vulnerability: Part B: Regional Aspects: Working Group II Contribution to the Fifth Assessment Report of the Intergovernmental Panel on Climate Change* (pp. 1–1820). Cambridge University Press. https://www.ipcc.ch/site/assets/uploads/2018/02/WGIIAR5-Chap21_FINAL.pdf

Bashir, F., Zeng, X., Gupta, H., & Hazenberg, P. (2017). A hydrometeorological perspective on the Karakoram anomaly using unique valley-based synoptic weather observations. *Geophysical Research Letters, 44*(20), 10–470.

Bayatvarkeshi, M., Zhang, B., Fasihi, R., Adnan, R. M., Kisi, O., & Yuan, X. (2020). Investigation into the effects of climate change on reference evapotranspiration using the HadCM3 and LARS-WG. *Water, 12*(3), 666.

Bookhagen, B., & Burbank, D. W. (2010). Toward a complete Himalayan hydrological budget: Spatiotemporal distribution of snowmelt and rainfall and their impact on river discharge. *Journal of Geophysical Research: Earth Surface, 115*(F3).

Bukovsky, M. S., & Mearns, L. O. (2020). Regional climate change projections from NA-CORDEX and their relation to climate sensitivity. *Climatic Change, 162*(2), 645–665.

Buytaert, W., Vuille, M., Dewulf, A., Urrutia, R., Karmalkar, A., & Célleri, R. (2010). Uncertainties in climate change projections and regional downscaling in the tropical Andes: Implications for water resources management. *Hydrology and Earth System Sciences, 14*(7), 1247–1258.

Chapagain, D., Dhaubanjar, S., & Bharati, L. (2021). Unpacking future climate extremes and their sectoral implications in western Nepal. *Climatic Change, 168*(1), 8. https://doi.org/10.1007/s10584-021-03216-8

Chen, H., Guo, J., Zhang, Z., & Xu, C.-Y. (2013). Prediction of temperature and precipitation in Sudan and South Sudan by using LARS-WG in future. *Theoretical and Applied Climatology, 113*, 363–375.

Dahri, Z. H., Ludwig, F., Moors, E., Ahmad, B., Khan, A., & Kabat, P. (2016). An appraisal of precipitation distribution in the high-altitude catchments of the Indus basin. *Science of the Total Environment, 548*, 289–306.

Daly, C. (2006). Guidelines for assessing the suitability of spatial climate data sets. *International Journal of Climatology: A Journal of the Royal Meteorological Society, 26*(6), 707–721.

De Souza, K., Kituyi, E., Harvey, B., Leone, M., Murali, K. S., & Ford, J. D. (2015). Vulnerability to climate change in three hot spots in Africa and Asia: key issues for policy-relevant adaptation and resilience-building research. *Regional Environmental Change, 15*, 747–753.

Ding, Y., Mu, M., Zhang, J., Jiang, T., Zhang, T., Wang, C., Wu, L., Ye, B., Bao, M., & Zhang, S. (2016). Impacts of climate change on the environment, economy, and society of China. In D. Qin, Y. Ding, & Mu Mu (Eds.), *Climate and environmental change in China: 1951–2012* (pp. 69–92). Springer

Ehret, U., Zehe, E., Wulfmeyer, V., & Liebert, J. (2012). Should we apply bias correction to global and regional climate model data? *HESS, 16*, 3391–3404.

FentaMekonnen, D., & Disse, M. (2018). Analyzing the future climate change of Upper Blue Nile River basin using statistical downscaling techniques. *Hydrology and Earth System Sciences, 22*(4), 2391–2408.

Forsythe, N., Fowler, H. J., Blenkinsop, S., Burton, A., Kilsby, C. G., Archer, D. R., Harpham, C., & Hashmi, M. Z. (2014). Application of a stochastic weather generator to assess climate change impacts in a semi-arid climate: The Upper Indus Basin. *Journal of Hydrology, 517*, 1019–1034. https://doi.org/10.1016/j.jhydrol.2014.06.031

Fotso-Nguemo, T. C., Diallo, I., Diakhaté, M., Vondou, D. A., Mbaye, M. L., Haensler, A., Gaye, A. T., & Tchawoua, C. (2019). Projected changes in the seasonal cycle of extreme rainfall events from CORDEX simulations over Central Africa. *Climatic Change, 155*(3), 339–357. https://doi.org/10.1007/s10584-019-02492-9

Fowler, H. J., & Archer, D. R. (2006). Conflicting signals of climatic change in the Upper Indus Basin. *Journal of Climate, 19*(17), 4276–4293.

Fowler, H. J., Blenkinsop, S., & Tebaldi, C. (2007). Linking climate change modelling to impacts studies: Recent advances in downscaling techniques for hydrological modelling. *International Journal of Climatology: A Journal of the Royal Meteorological Society, 27*(12), 1547–1578.

Gerlitz, L., Schickhoff, U., Scholten, T., & Böhner, J. (2016). Recent climate change over High Asia. In R. B. Singh, U. Schickhoff, & S. Mal (Eds.), *Climate change, glacier response, and vegetation dynamics in the Himalaya* (pp. 29–48). Springer.

Guijarro, J. A. (2018). *Homogenization of climatic series with Climatol*. Reporte técnico State Meteorological Agency (AEMET), Balearic Islands Office, Spain

Harding, R. J., Weedon, G. P., van Lanen, H. A. J., & Clark, D. B. (2014). The future for global water assessment. *Journal of Hydrology, 518*, 186–193.

Hashmi, M. Z., Shamseldin, A. Y., & Melville, B. W. (2011). Comparison of SDSM and LARS-WG for simulation and downscaling of extreme precipitation events in a watershed. *Stochastic Environmental Research and Risk Assessment, 25*(4), 475–484.

Hassan, M., Du, P., Mahmood, R., Jia, S., & Iqbal, W. (2019). Streamflow response to projected climate changes in the Northwestern Upper Indus Basin based on regional climate model (RegCM4. 3) simulation. *Journal of Hydro-Environment Research, 27*, 32–49.

Hasson, SUl. (2016). Future water availability from Hindukush-Karakoram-Himalaya Upper Indus Basin under conflicting climate change scenarios. *Climate, 4*(3), 40.

Hasson, S., Böhner, J., & Lucarini, V. (2017). Prevailing climatic trends and runoff response from Hindukush–Karakoram–Himalaya, upper Indus Basin. *Earth System Dynamics, 8*(2), 337–355.

IPCC. (2013). The physical science basis. *Contribution of Working Group I to the Fifth Assessment Report of the Intergovernmental Panel on Climate Change, 1535*, 2013.

Ismail, M. F., Naz, B. S., Wortmann, M., Disse, M., Bowling, L. C., & Bogacki, W. (2020). Comparison of two model calibration approaches and their influence on future projections under climate change in the Upper Indus Basin. *Climatic Change, 163*(3), 1227–1246. https://doi.org/10.1007/s10584-020-02902-3

Karam, S., Seidou, O., Nagabhatla, N., Perera, D., & Tshimanga, R. M. (2022). Assessing the impacts of climate change on climatic extremes in the Congo River Basin. *Climatic Change, 170*(3), 40. https://doi.org/10.1007/s10584-022-03326-x

Kavwenje, S., Zhao, L., Chen, L., & Chaima, E. (2022). Projected temperature and precipitation changes using the LARS-WG statistical downscaling model in the Shire River Basin, Malawi. *International Journal of Climatology, 42*(1), 400–415.

Khan, F., Pilz, J., Amjad, M., & Wiberg, D. A. (2015). Climate variability and its impacts on water resources in the Upper Indus Basin under IPCC climate change scenarios. *International Journal of Global Warming, 8*(1), 46–69.

Kilroy, G. (2015). A review of the biophysical impacts of climate change in three hotspot regions in Africa and Asia. *Regional Environmental Change, 15*(5), 771–782.

Kim, G., Cha, D.-H., Lee, G., Park, C., Jin, C.-S., Lee, D.-K., Suh, M.-S., Ahn, J.-B., Min, S.-K., & Kim, J. (2020). Projection of future precipitation change over South Korea by regional climate models and bias correction methods. *Theoretical and Applied Climatology, 141*(3), 1415–1429.

Kulkarni, A., Patwardhan, S., Kumar, K. K., Ashok, K., & Krishnan, R. (2013). Projected climate change in the Hindu Kush-Himalayan region by using the high-resolution regional climate model PRECIS. *Mountain Research and Development, 33*(2), 142–151.

Kumar, P., Saharwardi, M. S., Banerjee, A., Azam, M. F., Dubey, A. K., & Murtugudde, R. (2019). Snowfall variability dictates glacier mass balance variability in Himalaya-Karakoram. *Scientific Reports, 9*(1), 18192.

Lee, D.-K., & Cha, D.-H. (2020). Regional climate modeling for Asia. *Geoscience Letters, 7*(1), 1–12.

Luhunga, P. M., Kijazi, A. L., Chang'a, L., Kondowe, A., Ng'Ongolo, H., & Mtongori, H. (2018). Climate change projections for Tanzania based on high-resolution regional climate models from the coordinated regional climate downscaling experiment (CORDEX)-Africa. *Frontiers in Environmental Science, 6*, 122.

Lutz, A. F., Immerzeel, W. W., Kraaijenbrink, P. D. A., Shrestha, A. B., & Bierkens, M. F. P. (2016a). Climate change impacts on the upper Indus hydrology: Sources, shifts and extremes. *PLoS One, 11*(11), e0165630.

Lutz, A. F., ter Maat, H. W., Biemans, H., Shrestha, A. B., Wester, P., & Immerzeel, W. W. (2016b). Selecting representative climate models for climate change impact studies: An advanced envelope-based selection approach. *International Journal of Climatology, 36*(12), 3988–4005.

Maussion, F., Scherer, D., Mölg, T., Collier, E., Curio, J., & Finkelnburg, R. (2014). Precipitation seasonality and variability over the Tibetan Plateau as resolved by the High Asia Reanalysis. *Journal of Climate, 27*(5), 1910–1927.

MRI. (2015). Elevation-dependent warming in mountain regions of the world. *Nature Climate Change, 5*(5), 424–430.

Nepal, S., & Shrestha, A. B. (2015). Impact of climate change on the hydrological regime of the Indus, Ganges and Brahmaputra river basins: A review of the literature. *International Journal of Water Resources Development, 31*(2), 201–218.

Ougahi, J. H., Cutler, M. E. J., & Cook, S. J. (2022). Modelling climate change impact on water resources of the Upper Indus Basin. *Journal of Water and Climate Change, 13*(2), 482–504.

Palazzi, E., von Hardenberg, J., Terzago, S., & Provenzale, A. (2015). Precipitation in the Karakoram-Himalaya: A CMIP5 view. *Climate Dynamics, 45*, 21–45.

Pepin, N. C., Arnone, E., Gobiet, A., Haslinger, K., Kotlarski, S., Notarnicola, C., Palazzi, E., Seibert, P., Serafin, S., & Schöner, W. (2022). Climate changes and their elevational patterns in the mountains of the world. *Reviews of Geophysics, 60*(1), e2020RG000730.

Pomee, M. S., & Hertig, E. (2021). Temperature projections over the Indus River basin of pakistan using statistical downscaling. *Atmosphere, 12*(2), 195.

Pomee, M. S., & Hertig, E. (2022). Precipitation projections over the Indus River Basin of Pakistan for the 21st century

using a statistical downscaling framework. *International Journal of Climatology, 42*(1), 289–314.

Sarkar, J., Chicholikar, J. R., & Rathore, L. S. (2015). Predicting future changes in temperature and precipitation in arid climate of Kutch, Gujarat: analyses based on LARS-WG model. *Current Science, 109*, 2084–2093.

Semenov, M. A., Barrow, E. M., & Lars-Wg, A. (2002). *A stochastic weather generator for use in climate impact studies* (pp. 1–27). User Man Herts, UK.

Sha, J., Li, X., & Wang, Z.-L. (2019). Estimation of future climate change in cold weather areas with the LARS-WG model under CMIP5 scenarios. *Theoretical and Applied Climatology, 137*(3), 3027–3039.

Shah, M. I., Khan, A., Akbar, T. A., Hassan, Q. K., Khan, A. J., & Dewan, A. (2020). Predicting hydrologic responses to climate changes in highly glacierized and mountainous region Upper Indus Basin. *Royal Society Open Science, 7*(8), 191957.

Stott, P. A., & Kettleborough, J. A. (2002). Origins and estimates of uncertainty in predictions of twenty-first century temperature rise. *Nature, 416*(6882), 723–726.

Sunyer, M. A., Madsen, H., & Ang, P. H. (2012). A comparison of different regional climate models and statistical downscaling methods for extreme rainfall estimation under climate change. *Atmospheric Research, 103*, 119–128.

Tangang, F., Chung, J. X., Juneng, L., Salimun, E., Ngai, S. T., Jamaluddin, A. F., Mohd, M. S. F., Cruz, F., Narisma, G., & Santisirisomboon, J. (2020). Projected future changes in rainfall in Southeast Asia based on CORDEX–SEA multi-model simulations. *Climate Dynamics, 55*, 1247–1267.

Taylor, K. E. (2001). Summarizing multiple aspects of model performance in a single diagram. *Journal of Geophysical Research: Atmospheres, 106*(D7), 7183–7192.

Trzaska, S., & Schnarr, E. (2014). A review of downscaling methods for climate change projections. *United States Agency for International Development by Tetra Tech ARD*, pp. 1–42.

Wake, C. P. (1989). Glaciochemical investigations as a tool for determining the spatial and seasonal variation of snow accumulation in the central Karakoram, northern Pakistan. *Annals of Glaciology, 13*, 279–284.

Zhang, X., & Yang, F. (2004). RClimDex (1.0) user manual. *Climate Research Branch Environment Canada, 22*, 13–14.